Float zone growth and anisotropic spectral properties of Nd:$LaVO_4$ single crystals

Shohei Yomogida[1], Mikio Higuchi[1], Takayo Ogawa[2], Satoshi Wada[2], Junichi Takahashi[1]

[1] Faculty of Engineering, Hokkaido University, Sapporo 060-8628, Japan
[2] RIKEN, Wako 351-0198, Japan

Abstract

Nd:$LaVO_4$ single crystals were successfully grown by the floating zone method and their optical properties along each optic elasticity axis were investigated. The crystals grown at 10mm/h in air did not contain any macroscopic defects for Nd-concentrations up to 5 at%. The optic elasticity axes were determined by the conoscopic figures with a polarizing microscope. The absorption cross-section along the *Z*-axis was 2.6×10^{-20} cm^2 near 800 nm and the FWHM was 20 nm. The absorption cross-sections along other directions were much the same as that along the *Z*-axis. The fluorescence lifetime of the 5 at%-doped crystal was approximately 80 μs. All the polarized fluorescence spectra of the Nd:$LaVO_4$ single crystal had a broadened band around 1060 nm with FWHMs of 7-10 nm, which are wide enough to generate femtosecond order pulses.

Key word

A2. Floating zone technique

B1. Vanadates

B3. Solid state lasers

1. Introduction

Ultra-short pulse lasers are used in a variety of applications, such as ultra-fine processing and ultraprecise measurements [1-4]. For the mode lock type of short pulse laser, pulse duration is determined by the gain bandwidth of the laser medium on the basis of Heisenberg's uncertainty principle [5];

$$\Delta t \times \Delta E \geq h/4\pi \qquad (1)$$

where E is energy, t is time and h is Planck's constant. From this principle, to achieve small Δt, namely ultra-short pulse, it is necessary to use a material having large ΔE, i.e. a broad emission band.

Ti:sapphire is currently used as a gain medium for femtosecond lasers since it has a broad emission band from 700 nm to 900 nm, but it cannot be pumped with a commercially available laser diode (LD) [4, 6-8]. Accordingly, the present femtosecond laser system is very expensive and of large scale, and thus there has been an increasing interest in research for LD-pumped ultra-short pulse laser materials [9-17].

Yb-doped crystals are one of the candidates for LD-pumped ultra-short pulse laser media. Yb-laser materials have been extensively investigated, since they have broad absorption and emission bands due to the transition between the ground state of $^2F_{7/2}$ and the excited state of $^2F_{5/2}$. However, they are known as a quasi-three-level laser on the basis of the Stark splitting of the ground state, requiring intensive pumping and efficient heat removal to attain population inversion, and the threshold is consequently increased [10-16].

In contrast, Nd-doped crystals are well known as efficient LD-pumped laser media, especially Nd-doped vanadates. Nd:YVO_4 and Nd:$GdVO_4$, are extensively investigated since they have large absorption and emission cross-sections; however, the fluorescence band widths of these materials are too narrow to achieve ultra-short pulse lasers of subpicosecond order [17-26]. In recent reports, it has been clarified that a host crystal that can provide Nd^{3+} with a large substitution site shows a

broadened emission band [27, 28].

$LaVO_4$ crystallizes in the monoclinic monazaite type structure with the space group of $P2_1/n$, in which the La^{3+} is of 9-fold oxygen coordination [29]. According to Shannon [30], the ionic radii of La^{3+} and Nd^{3+} for 9-fold coordination are 1.216 Å and 1.163 Å, respectively. Therefore, $LaVO_4$ can provide Nd^{3+} with large sites, and a broadened emission band is expected. Nd:$LaVO_4$ single crystals have already been grown by the Czochralski method and clarified to have broadened absorption and emission bands [31]; however, detailed characterization of optical properties such as the anisotropy of absorption and emission spectra and their polarization dependence is not reported. Since the $LaVO_4$ crystal is optically biaxial, it has three principal axes (*X*-, *Y*-, and *Z*-axis) of the optical indicatrix [32], which should be determined.

We have demonstrated that the floating zone method is an excellent technique to grow high quality vanadate single crystals [18-23, 33-37]. The most outstanding advantage of this method makes it possible to grow $REVO_4$ crystals under a high oxygen partial pressure such as a pure oxygen flow since no crucible is necessary, and the decomposition and vaporization of vanadium oxides are consequently suppressed resulting in macroscopic defect-free crystals.

In this study, we grew Nd:$LaVO_4$ single crystals with high optical quality by the floating zone method and investigated their anisotropic optical properties on the basis of the three principal axes.

2. Experimental procedure

$LaVO_4$ single crystals doped with 0.5-5 at% Nd were grown by the floating zone method. Feed rods for the floating zone growth were prepared via a conventional ceramic process. Powders of La_2O_3 (4N), V_2O_5 (4N) and Nd_2O_3 (3N) were mixed at the stoichiometric composition in an agate mortar with the aid of ethanol. The mixed powder was calcined at 650 ˚C for 10 h in air. After grinding, the powder was formed into a rod under a hydrostatic pressure of 100 MPa, and then sintered at 1200 ˚C for 10 h in air.

The crystals were grown in an image furnace with double ellipsoidal mirrors (NEC Machinery SC-N35HD-L), in which two halogen lamps of 1.5 kW were used as a heat source. Crystal growth was performed in the typical manner of the floating zone method [18-23, 33-37]. Since a single crystalline seed was not available, a sintered rod was used as a seed crystal in the initial stage of this study. By using a neck-down process, a Nd:$LaVO_4$ single crystal was easily obtained. A *Z*-axis seed crystal was finally prepared by the observation of conoscopic figures with a polarizing microscope. Other growth conditions were as follows: growth rate was 10 mm/h; rotation rate was 5 rpm for the feed rod and 40 rpm for the seed crystal; atmosphere was air.

After post-growth annealing at 1500 ˚C for 10 h in air, the crystals were cut and polished perpendicular to the growth direction to check the crystal quality from the orthoscopic figure with the polarizing microscope, followed by conoscopic observation to determine the optic elasticity axes *X*, *Y* and *Z*. Electron probe microanalysis (EPMA) was performed to investigate the distribution of dopant concentration along the growth axis. The principal refractive indices (α, β, γ) of $LaVO_4$ were measured by the Duc de Chaulnes method. Absorption and emission spectra were measured with a spectrophotometer and a monochromator, respectively.

3. Results and discussion

3.1 Crystal growth and characterization

Crack-free, transparent Nd:$LaVO_4$ single crystals were successfully grown at a growth rate of 10 mm/h by the floating zone method. A higher growth rate resulted in cracking of the crystals. In the case of the zircon-type of Nd-doped orthovanadate, crack-free crystals with a similar diameter could be grown even at 30 mm/h by the floating zone method [22, 23]. The lower symmetry of the monoclinic monazite structure than the tetragonal zircon-type may be responsible for larger thermal stresses resulting in cracking of the Nd:$LaVO_4$ single crystals.

A Nd:$LaVO_4$ (4 at%) single crystal grown by the floating zone method is shown in fig. 1. The typical dimensions of the grown crystals were about 5 mm in diameter and 40 mm length. Every as-grown crystal was transparent and colored purple, which is the intrinsic color of Nd-doped crystals. Darker purple crystals were obtained with increasing Nd-concentration; however, the color of Nd:$LaVO_4$ is appreciably lighter, which reflects relatively a small absorption cross section of this crystal as discussed later.

The graph in Fig. 2 presents line profiles of the Nd-concentration along the growth direction analyzed by EPMA. The Nd-concentration was nearly uniform from the initial stage of the growth, which means that the effective distribution coefficient of Nd in $LaVO_4$ is close to unity. The ionic radius of Nd^{3+} is only 5% smaller than that of La^{3+} for 9-fold coordination; therefore Nd^{3+} can easily substitute in the La^{3+} site.

Fig. 3 shows typical polarizing microphotographs of the Nd:$LaVO_4$ single crystal. As shown in the orthoscopic figure (Fig. 3(a)), the grown crystal has no macroscopic defects such as inclusions and low-angle grain boundaries. Thus Nd:$LaVO_4$ single crystals having high optical uniformity were obtained by the floating zone method for the Nd-concentration of up to 5 at%.

A conoscopic figure (Fig. 3(b)) was observed for the same crystal shown in fig. 3(a) to determine the optical elasticity axes of Nd:$LaVO_4$. $LaVO_4$ crystallizing in the monoclinic crystal system is an optically biaxial crystal, in which refractive indices are based on the biaxial indicatrix shown in Fig. 4, where *X*-, *Y*-, and *Z*-axes are called as optic elasticity axes, and principal refractive indices (α, β, and γ) are defined along these axes. Thus the optical properties of a biaxial crystal should be measured along the optic elasticity axes rather than along the crystallographic axes. In a monoclinic crystal, one of the optic elasticity axes is parallel to the crystallographic *b*-axis, and the other two do not necessarily correspond to the crystallographic axes. In the case of $LaVO_4$, it was confirmed by XRD that the *X*-axis is inclined at about 15 degrees to the *a*-axis, and *Y*- and *Z*-axis are parallel to the *b*- and *c*-axis, respectively. The cross-shaped isogyres shown in Fig. 3(b) indicates that the plane observed is perpendicular to the *Z*-axis, and directions of isogyres correspond to those of

X-axis and *Y*-axis. A rectangular crystal with each plane cut perpendicular to the *X*-, *Y*- and *Z*- axes, was prepared and anisotropic spectroscopic properties were evaluated by using this sample.

3.2 Spectroscopic properties

Fig. 5 shows the absorption spectrum of the Nd 4 at% doped $LaVO_4$ single crystal in the wavelength region of 700 to 950 nm. There are three strong absorption bands around 750, 800 and 885 nm, corresponding to the transitions of $^4I_{9/2} \rightarrow {}^4S_{3/2}+{}^4F_{7/2}$, $^4I_{9/2} \rightarrow {}^2H_{9/2}+{}^4F_{5/2}$, $^4I_{9/2} \rightarrow {}^4F_{3/2}$, respectively. In this absorption spectrum, the absorption band at about 800 nm is the most important for a LD-pumped laser since the emission wavelength of a commercially available LD is about 808 nm. In the wavelength region of 750 to 850 nm, the polarized absorption spectra along each optic elasticity axis was measured, as shown in Fig. 6. Since all the spectra show a broadened absorption band around 800 nm with FWHM~20 nm, they are suitable for LD-pumping. The absorption spectra along *X*- and *Y*-axes are polarization dependent; the absorption of the light vibrating parallel to the *Z*-axis is larger than those parallel to the *Y*- and *X*-axis. On the other hand, the spectrum measured along the *Z*-axis shows little polarization dependence. This polarization dependence is correlated with the principal refractive indices (α: ~2.09, β: ~2.09, and γ: ~2.22), which were roughly estimated by the Duc de Chaulnes method using an optical microscope. Despite an optically biaxial crystal, the refractive indices, α and β, are virtually equal in $LaVO_4$. Similar results of the refractive indices are reported for the natural monazite-type of minerals, although they are not vanadates but phosphates [38]. Monazite and zircon have a common structural characteristic, that is, coordination polyhedral of VO_4 and REO_9 (in monazite) or REO_8 (in zircon) form a chain along the *c*-axis in both structures [39]. The light vibrating parallel to the *c*-axis may strongly interact with the chains, and its refractive index and absorption cross section are expected to be larger than those vibrating perpendicular to the *c*-axis.

The spectra in fig 6 also indicate that Nd:$LaVO_4$ has little anisotropy of absorption and the

absorption cross-section at peak is about 2.5×10^{-20} cm^2 along any direction. This absorption cross-section is relatively small as compared with those of Nd:$REVO_4$ (RE=Gd, Y, Lu) single crystals with the tetragonal zircon type of structure. The small absorption cross section may reflect that Nd^{3+} ions have a variety of coordination environments in the larger La-sites although the differences in the environments are very small.

Fig. 7 shows the polarized emission spectra along each optic elasticity axis of the 4 at% doped Nd:$LaVO_4$ single crystals in the region 1000 to 1150 nm. This fluorescence band corresponding to the $^4F_{3/2}\rightarrow{}^4I_{11/2}$ transition, which is the main laser transition for Nd-laser oscillation, includes two peaks by Stark splitting. The emission bandwidth around 1064 nm is ~7-10 nm, which as wide as that of Yb:YAG, with which ultra-short pulse operation of subpico second was achieved [15, 16]. These broad emission bands are due to substitution of Nd^{3+} on the larger La-site as mentioned above. The polarization dependence of emission spectra is the same as that of absorption spectra, that is, the polarization dependence along the *Z*-axis is the smallest in both cases. Considering the absorption and emission spectra, since there is an advantage of little polarization dependence of absorption, the gain path should be made along the *Z*-axis, when a Nd:$LaVO_4$ single crystal is used in an end-pump type of laser cavity.

A fluorescence decay curve was measured for all the different Nd-concentrations, and a typical decay curve of 4 at% crystal is shown in Fig. 8. Since there are various states of Nd^{3+} in the La-site, it is not completely linear in a semilogarithmic plot. However, the difference in the states of Nd^{3+} is negligible; the fluorescence lifetime can accordingly be calculated by approximating the decay curve as a single component.

The calculated lifetimes of 0.5-5 at% doped-Nd:$LaVO_4$ are plotted as shown in Fig. 9. The fluorescence lifetime of the $^4F_{3/2}$ level decreases with increasing Nd-concentration because of concentration quenching; however, lifetimes of all crystals (80-160 μs) were long enough for lasing. Zhang et al. reported that the lifetime of the Czochralski-grown Nd:$LaVO_4$ with a Nd-concentration of 3.5 at% was 137μs, which is comparable to that of the Nd 2 at% crystal grown by the floating

zone method. However, the Nd-concentration of the Czochralski-grown crystal was just a nominal one and the actual concentration may be much lower than 3.5 at%, taking account the segregation coefficient. Since Nd-doped crystals can be grown up to 5 at% without deterioration of crystal quality, the drawback of the small absorption cross-section can be compensated by using 3-5 at% Nd-doped crystals.

Investigation of lasing characteristic of the Nd:$LaVO_4$ single crystals, such as the lasing threshold, the conversion efficiency, and the laser spectrum band width, is underway aiming for the fabrication of an LD-pumped ultra-short pulse system.

4. Conclusions

Nd-doped $LaVO_4$ single crystals were successfully grown by the floating zone method and their anisotropic optical properties were investigated with a goal of a new type of LD-pumped ultra-short pulse lasers. Every crystal was free from any macroscopic defects and had optical and compositional homogeneity. The absorption cross-section along the *Z*-axis was 2.6×10^{-20} cm^2 near 800 nm and the FWHM was 20 nm. The absorption cross-sections along other directions were much the same as that along the *Z*-axis, along which the polarization dependence is negligible. This result implies that pumping along the *Z*-axis is the best way for the end-pump type of laser cavity. All the polarized fluorescence spectra of the Nd:$LaVO_4$ single crystal had a broadened band around 1060 nm with FWHMs of 7-10 nm, which are wide enough to generate femtosecond order pulses. The fluorescence lifetime of 5 at%-doped crystal was about 80 μs, which is sufficient to achieve the laser oscillation. The absorption cross-section of Nd:$LaVO_4$ is relatively small, but this drawback can be compensated by 3-5 at% Nd-doping, which is possible by the floating zone method without deterioration of the crystal quality and significant decrease in fluorescence lifetime. Therefore, Nd:$LaVO_4$ single crystals are one of the promising materials for LD-pumped ultra-short pulse lasers.

References

[1] B.N. Chichkov, C. Momma, S. Nolte, F. von Alvensleben, A. Tünnermann, Applied Physics A 63 (1996) 109

[2] J. Qiu, K. Miura, K. Hirao, Journal of Non-Crystalline Solids 354 (2008) 1100

[3] J. Zhao, B. Huettner, A. Menschig, Optics & Laser Technology 33 (2001) 487

[4] D. Bruneel, G. Matras, R. Le Harzic, N. Huot, K. König, E. Audouard, Optics and Lasers in Engineering 48 (2010) 268

[5] P. Busch, T. Heinonen, P. Lahti, Physics Reports 452 (2007) 155

[6] P. Dufour, G. Rousseau, M. Piché, N. McCarthy, Optics Communications 247 (2005) 427

[7] U. Morgner, F.X. Kärtner, S.H. Cho, Y. Chen, H. A. Haus, J. G. Fujimoto, E.P. Ippen, V. Scheuer, G. Angelow, T. Tschudi, Optics Letters 24 (1999) 411

[8] M.G. Kovalsky, A.A. Hnilo, A. Libertun, M.C. Marconi, Optics Communications 192 (2001) 333

[9] E. Sorokin, I. T. Sorokina, E. Wintner, Applied Physics B 72, (2001) 3

[10] K. Sueda, S. Kawato, T. Kobayashi, Laser Physics Letters 5 (2008) 271

[11] A.A. Demidovich, A.N. Kuzumin, G.I. Ryabtsev, M.B. Danailov, W. Strek, A.N. Titov, Journal of Alloys and Compounds 300-301 (2000) 238

[12] F. Druon, F. Balembois, P. Georges, Optics Express 12 (2004) 5005

[13] A. Malinowski, A. Piper. J.H.V. Price, K. Furusawa, Y. Jeong, J. Nilsson, D.J. Richardson, Optics Letters 29 (2004) 2073

[14] F. Druon, F. Balembois, P. Georges, A. Brun, A. Courjaud, C. Hönninger, F. Salin, A. Aron, F. Mougel, G. Aka, D. Vivien, Optics Letters 25 (2000) 423

[15] C. Hönninger, G. Zhang, U. Keller, A. Giesen, Optics Letters 20 (1995) 2402

[16] H. Yoshioka, S. Nakamura, T. Ogawa, S. Wada, Optics Express 18 (2010) 1479

[17] M. Montes, V. de las Heras, D. Jaque, Optics Materials 28 (2006) 408

[18] T. Shonai, M. Higuchi, K. Kodaira, T. Ogawa, S. Wada, H. Machida, Journal of Crystal Growth 241 (2002) 159

[19] M. Higuchi, H. Sagae, K. Kodaira, T. Ogawa, S. Wada, H. Machida, Journal of Crystal Growth 264 (2004) 284

[20] T. Shonai, M. Higuchi, K. Kodaira, Journal of Crystal Growth 233 (2001) 477

[21] T. Shonai, M. Higuchi, K. Kodaira, Materials Research Bulletin 35 (2000) 225

[22] T. Ogawa, Y. Urata, M. Higuchi, J. Takahashi, C. Leong, J. Morikawa, T. Hashimoto, S. Wada, Applied Physic Express 2 (2009) 012501

[23] T. Ogawa, Y. Urata, S. Wada, K. Onodera, H. Machida, H. Sagae, M. Higuchi, K. Kodaira, Optical Letters 28 (2003) 2333

[24] T. Jensen, V.G. Ostroumov, J.P. Meyn, G. Huber, A.I. Zagumennyi, I.A. Shcherbakov, Applied Physics B 58 (1994) 373

[25] T. Taira, A. Mukai, Y. Nozawa, T. Kobayashi, Optical Letters 16 (1991) 1995

[26] Z. Wang, H. Zhang, F. Xu, D. Hu, X. Xu, J. Wang, Z. Shao, Laser Physics Letters 5 (2008) 25
[27] V.G. Ostroumov, G. Huber, A.I. Zagumennyi, Yu.D. Zavartsev, P.A. Studenikin, I.A. Shcherbakov, Optics Communications 124 (1996) 63
[28] H. Zhang, X. Meng, L. Zhu, C. Wang, P. Wang, H. Zhang, Y.T. Chow, J. Dawes, Journal of Crystal Growth 193 (1998) 370
[29] C.E. Rice, W.R. Robinson, Acta Crystal B32 (1976) 2232
[30] R.D. Shannon, Acta Crystal A32 (1976) 751
[31] L. Zhang, Z. Hu, Z. Lin, G. Wang, Journal of Crystal Growth 260 (2004) 460
[32] G.P. Misson, Ophthalmic and Physiological Optics 30 (2010) 834
[33] M. Higuchi, K. Kodaira, Y. Urata, S. Wada, H. Machida, Journal of Crystal Growth 265 (2004) 487
[34] A. Wu, S. Pan, J. Xu, T. Ogawa, S. Wada, M. Higuchi, K. Kodaira, Journal of Crystal Growth 311 (2009) 888
[35] R. Lisiecki, P. Solarz, G. Dominiak-Dzik, W. Ryba-Romanowski, M. Sobczyk, P. Černý, J. Šulc, H. Jelínková, Y. Urata, M. Higuchi, Physical Review B 74 (2006) 035103
[36] M. Higuchi, T. Shimizu, J. Takahashi, T. Ogawa, Y. Urata, T. Miura, S. Wada, H. Machida, Journal of Crystal Growth 283 (2005) 100
[37] M. Higuchi, R. Sasaki, J. Takahashi, Journal of Crystal Growth 311 (2009) 4549
[38] C.M. Gramaccioli, T.V. Segalstad, American Mineralogist 63 (1978) 757
[39] A. Meldrum, L.A. Boatner, R.C. Ewing, Physical Review B 56 (1997) 13805

Figure captions

Fig. 1. Float zone grown Nd:$LaVO_4$ single crystal (Nd: 4 at%).

Fig. 2. Distribution of Nd-concentration along the growth direction in the Nd:$LaVO_4$ single crystal (Nd: 4 at%).

Fig. 3. Polarizing microphotographs of vertical cross-sections of 4 at% doped Nd:$LaVO_4$ single crystals: (a) orthoscopic figure; (b) conoscopic figure.

Fig. 4. Optical indicatrix for optically biaxial crystals.

Fig. 5. Absorption spectrum of the Nd:$LaVO_4$ single crystal along *Z*-axis in the wavelength region of 700 to 950 nm.

Fig. 6. Polarized absorption spectra of the Nd:$LaVO_4$ single crystal along each optic elasticity axis.

Fig. 7. Polarized emission spectra of the Nd:$LaVO_4$ (4 at%) single crystal along each optic elasticity axis. (λ_{ex}: 809 nm)

Fig. 8. Fluorescence decay curve of Nd:$LaVO_4$ (4 at%) single crystal. (λ_{ex}: 809 nm, λ_{em}: 1064 nm)

Fig. 9. Nd-concentration dependence of the fluorescence lifetime of the Nd:$LaVO_4$ single crystals.

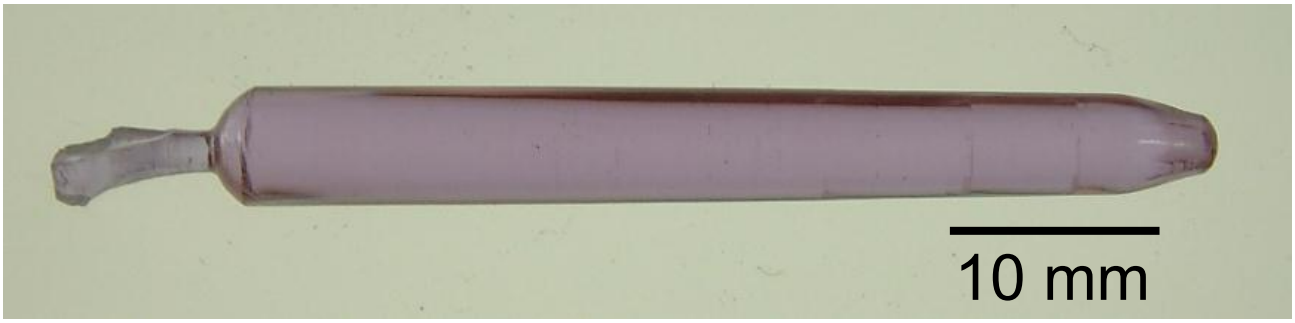

Fig. 1. Float zone grown Nd:$LaVO_4$ single crystal (Nd: 4 at%).

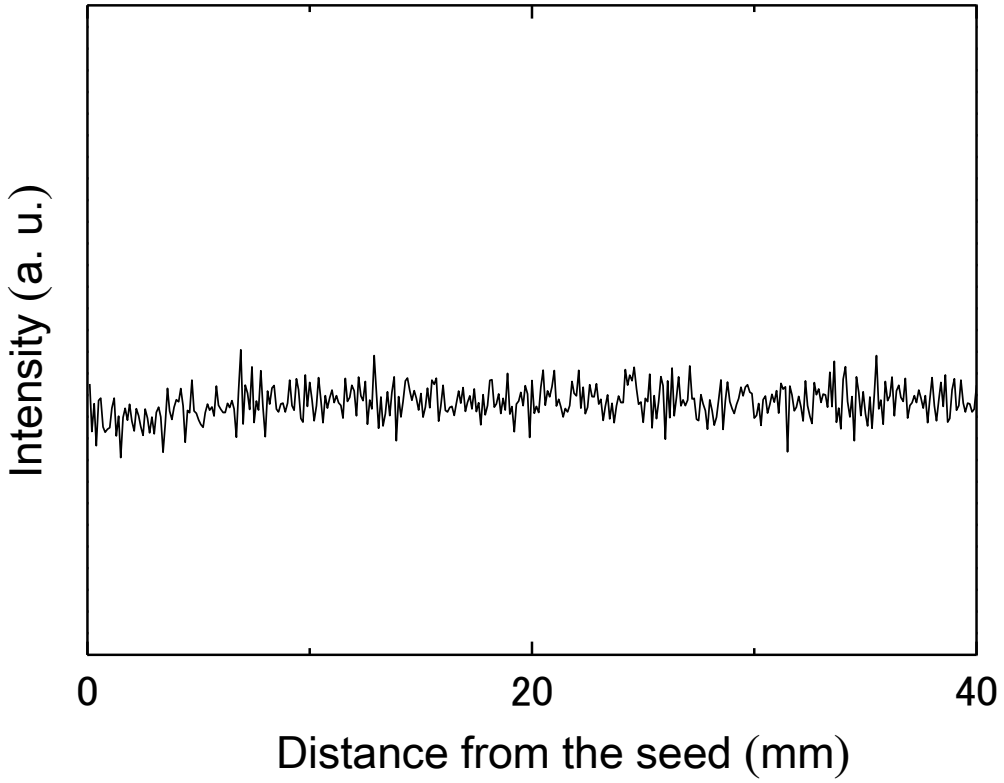

Fig. 2. Distribution of Nd-concentration along the growth direction in the Nd:$LaVO_4$ single crystal (Nd: 4 at%).

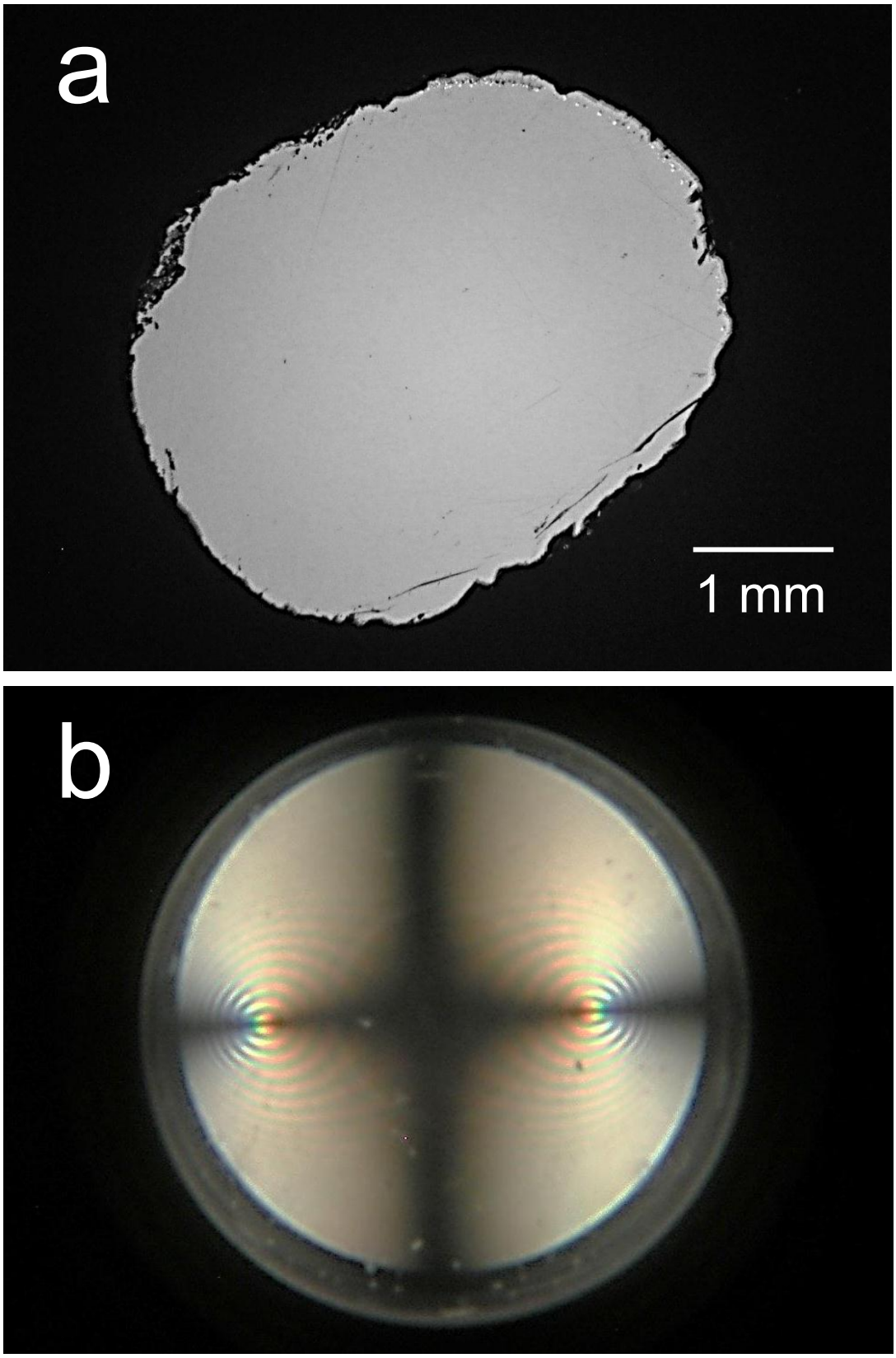

Fig. 3. Polarizing microphotographs of vertical cross-sections of 4 at% doped Nd:$LaVO_4$ single crystals: (a) orthoscopic figure; (b) conoscopic figure.

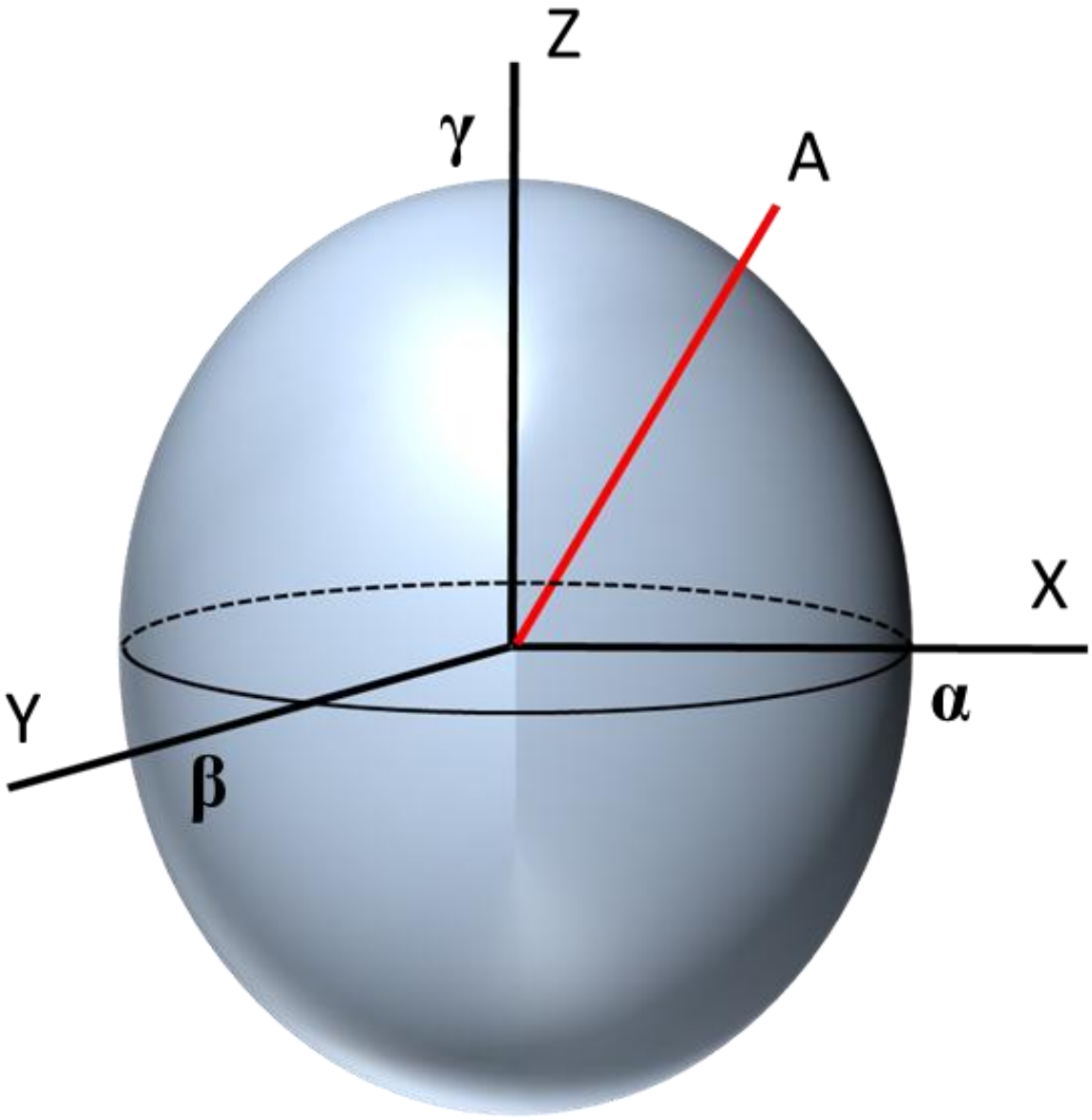

Fig. 4. Optical indicatrix for optically biaxial crystals.

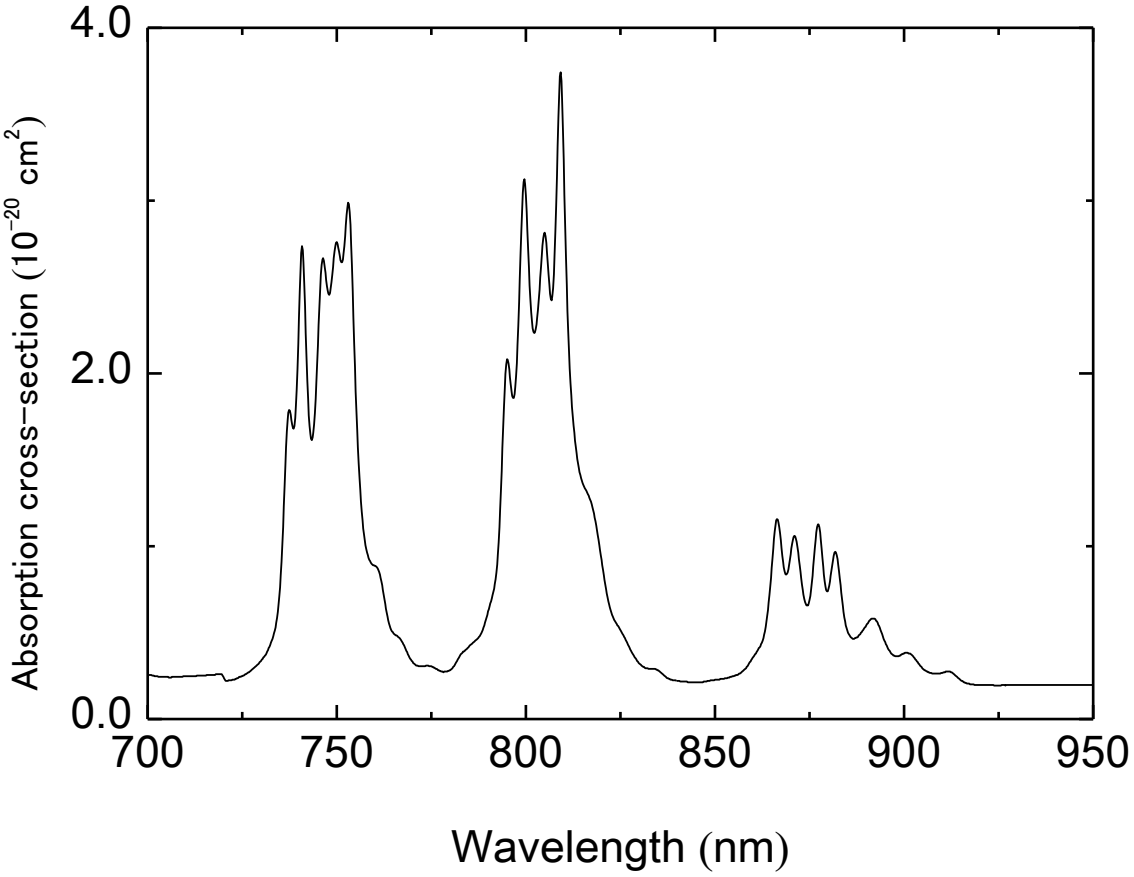

Fig. 5. Absorption spectrum of the Nd:$LaVO_4$ single crystal along *Z*-axis in the wavelength region of 700 to 950 nm.

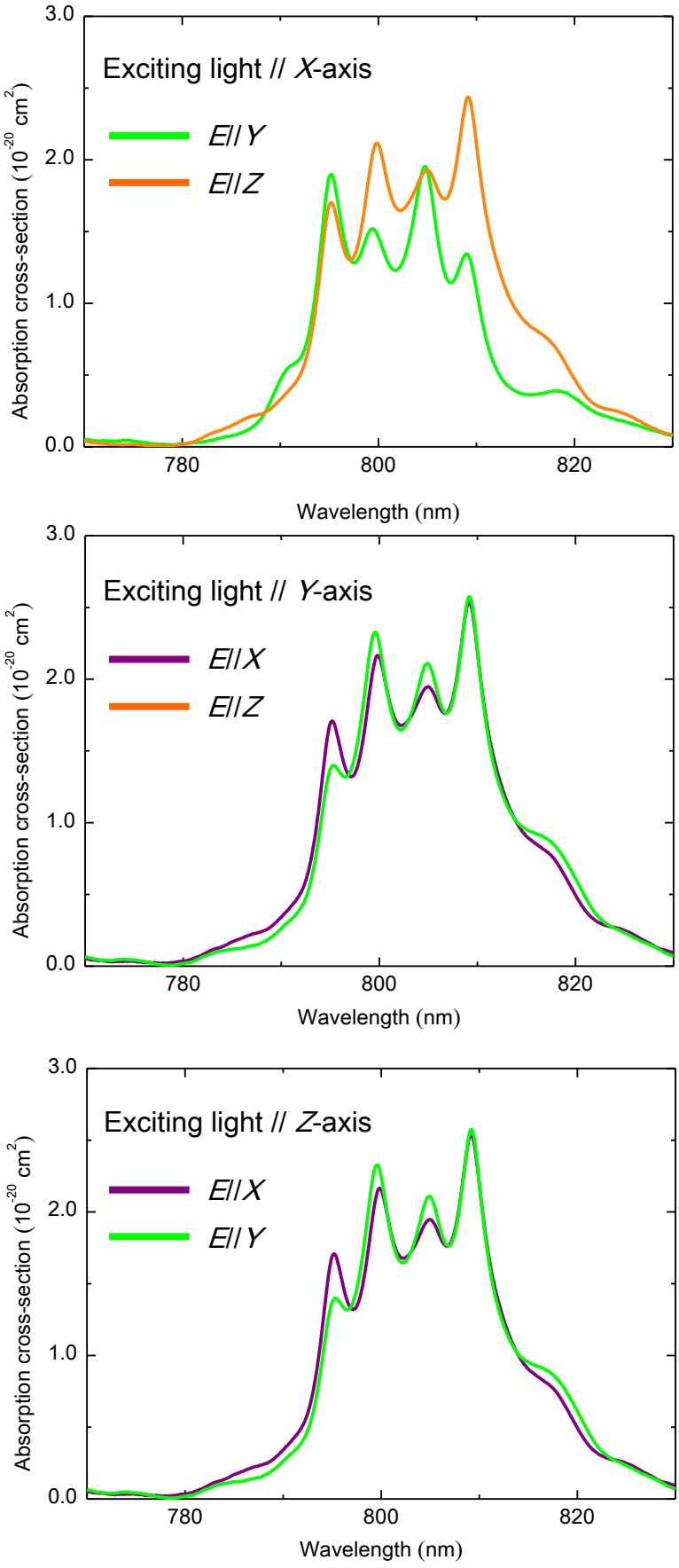

Fig. 6. Polarized absorption spectra of the Nd:$LaVO_4$ single crystal along each optic elasticity axis.

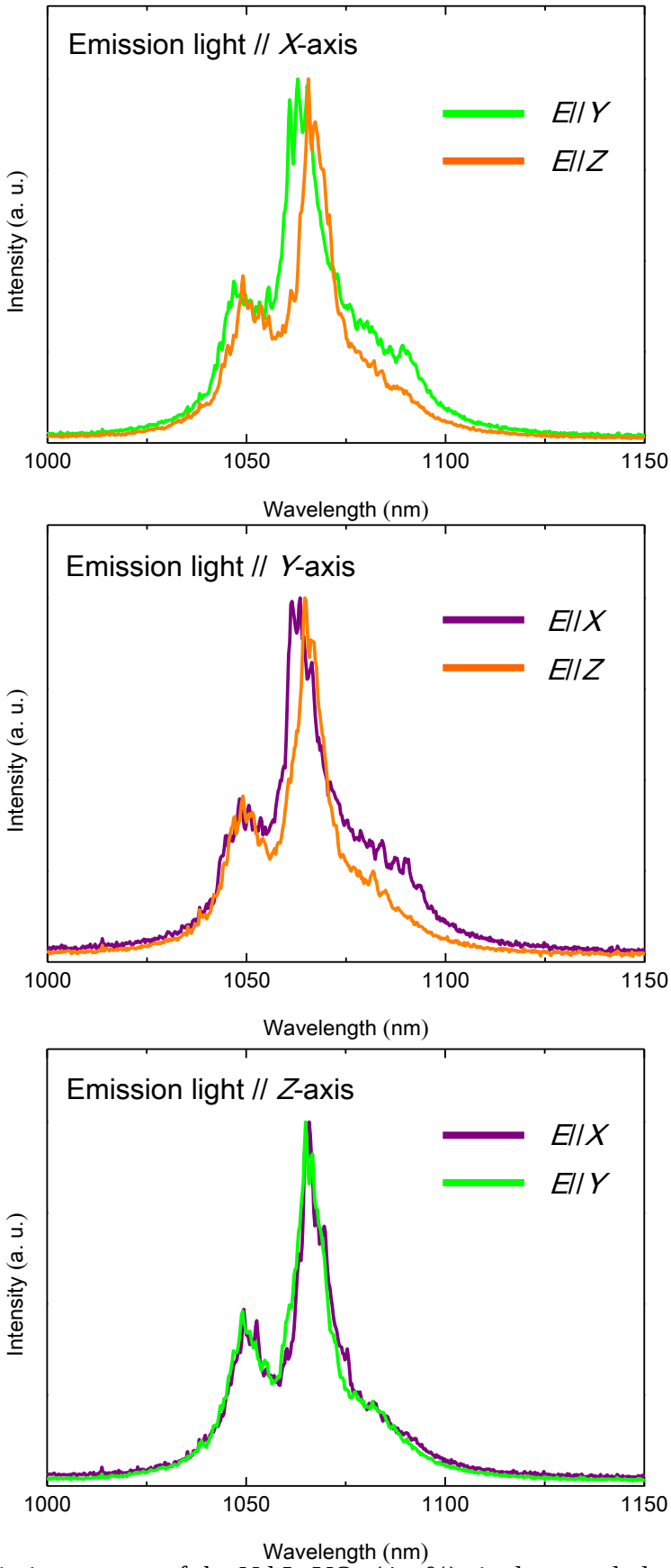

Fig. 7. Polarized emission spectra of the Nd:$LaVO_4$ (4 at%) single crystal along each optic elasticity axis. (λ_{ex}: 809 nm)

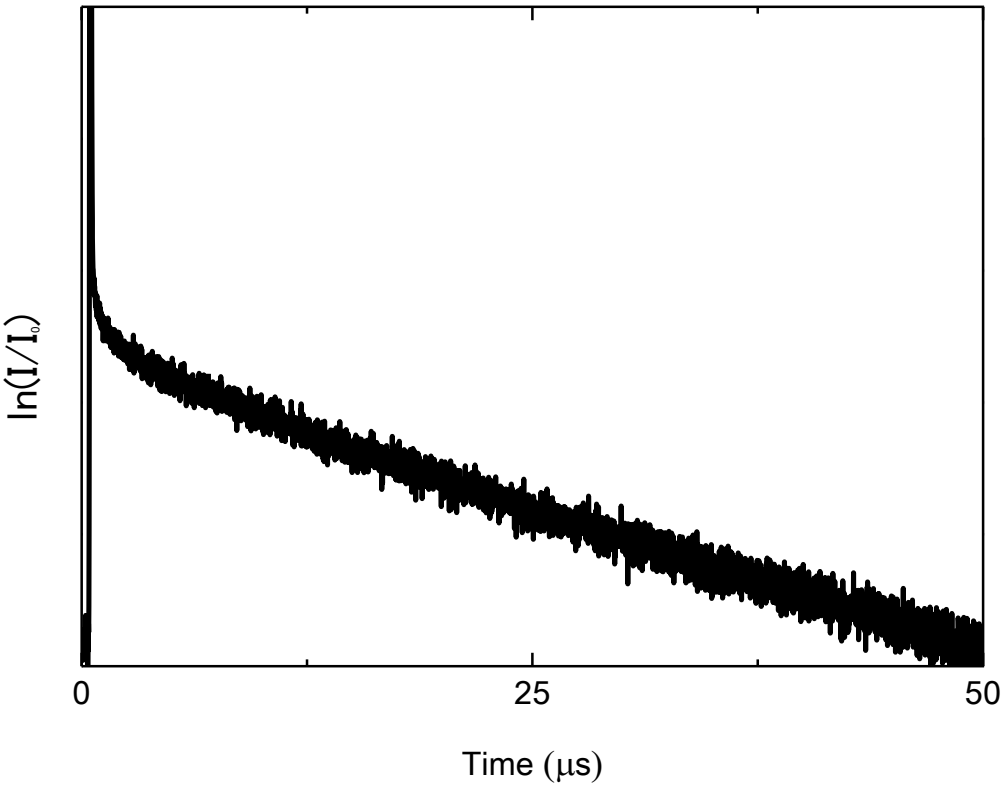

Fig. 8. Fluorescence decay curve of Nd:$LaVO_4$ (4 at%) single crystal. (λ_{ex}: 809 nm, λ_{em}: 1064 nm)

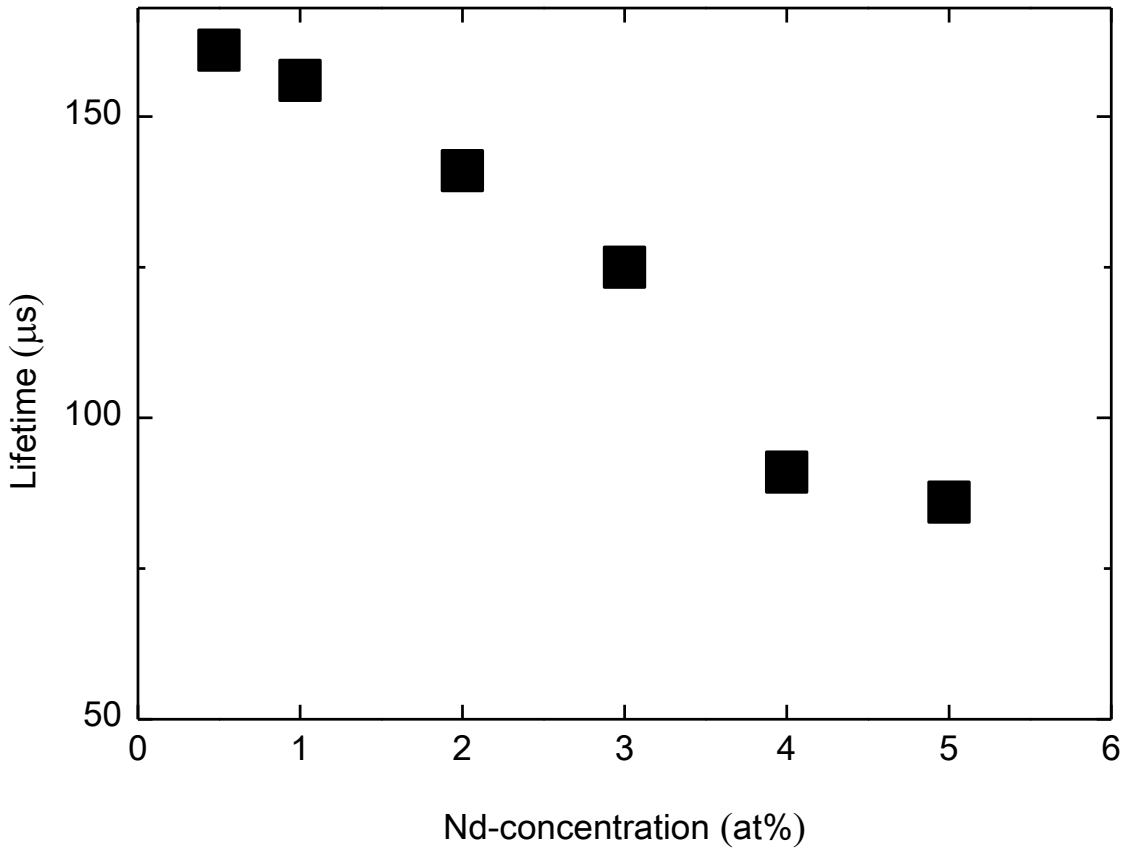

Fig. 9. Nd-concentration dependence of the fluorescence lifetime of the Nd:$LaVO_4$ single crystals.